Chemical Engineering Journal 463 (2023) 142307

Contents lists available at ScienceDirect

Chemical Engineering Journal

journal homepage: www.elsevier.com/locate/cej

Self-healing, tough, red-to-near-infrared (NIR) luminescent organohydrogels derived from supramolecular assemblies of common aggregation-induced emissive luminogens

Shuhui An [a,b,1], Xiaoyi Zhang [c,1], Muqing Si [a,b], Huihui Shi [a,b], Peng Wei [c,*], Jianwei Shen [d,*], Wei Lu [a,b,*], Tao Chen [a,b]

[a] Key Laboratory of Marine Materials and Related Technologies, Zhejiang Key Laboratory of Marine Materials and Protective Technologies, Ningbo Institute of Materials Technology and Engineering, Chinese Academy of Sciences, Ningbo 315201, China
[b] School of Chemical Sciences, University of Chinese Academy of Sciences, 19A Yuquan Road, Beijing 100049, China
[c] Department of Plastic and Reconstructive Surgery, Ningbo First Hospital, Ningbo 315010, China
[d] Department of Gastroenterology, Ningbo Medical Center Lihuili Hospital, 1111 Jiangnan Road, Ningbo 315000, China

ARTICLE INFO

Keywords:
Polymeric gel
Aggregation-induced emission
Supramolecular assembly
Red-to-NIR luminescence
Organohydrogel

ABSTRACT

Luminescent polymeric gels (LPGs) are promising for wide high-tech applications due to their hydrated state, tunable emission and similarity to bio-tissues. However, most LPGs only exhibit visible luminescence below 630 nm and cannot emit the preferred near-infrared (NIR) luminescence (650 ~ 900 nm). Herein, we report red-to-NIR aggregation-induced emissive LPGs based on supramolecular co-assemblies of cationic terpyridine platinum (II) luminogen (TPY-Pt) and anionic alginate (Alg) with unexpected large red emission shift (~100 nm). Combined analyses of UV–Vis/emission spectra, transmission electron microscopy (TEM), dynamic light scattering (DLS), zeta potential results, and density functional theory (DFT) calculations suggested that such large red-shifted emission derived from coupling of the dyes' transition dipole moments in TPY-Pt/Alg co-assemblies. Interestingly, red-to-NIR luminescence was well-preserved after TPY-Pt/Alg co-assemblies were physically incorporated into crosslinked poly(vinyl alcohol) (PVA) networks. Consequently, PVA organohydrogels and hydrogels with red-to-NIR emission bands respectively centered at 698 nm and 708 nm were obtained. After further mechanical training to induce anisotropic orientational structures, these PVA organohydrogels were able to bear a high stress of 1.4 MPa. They also had pH-responsive emission, self-healing and remolding capacities, and biocompatibility. The developed red-to-NIR luminescent organohydrogels with these integrated merits have been seldom reported and are expected to find many potential applications.

1. Introduction

Luminescent polymeric gels (LPGs) are an important type of luminescent soft matters with crosslinked 3D polymer networks swollen by solvent (e.g., water, ethylene glycol, or their mixtures) [1,2]. They can thus combine the advantages of luminescent materials and polymeric gels, including tunable emission, hydrated state and flexible nature [3,4], which makes them have broad applications such as optical sensing [5–7], bio-imaging [8], visual electronics [9] and soft actuators/robotics [10,11]. Usually, most LPGs are directly prepared by introducing the readily available luminogens (e.g., organic luminogens [12–14], metal complexes [15,16], luminescent proteins [17] or nanoparticles [18,19]) that are soluble in the solvent into crosslinked polymer matrix by the approaches of either physical blending or chemical bonding. But LPGs can also be obtained from the insoluble luminogens, through pre-polymerizing them into soluble polymer chains [20], or pre-designing microstructures (e.g., micelles or fibers) that can accomdate them [21,22]. Based on these well-established strategies, a large number of elegant luminescent gels have been reported and aroused global research interests [23,24]. Nevertheless, most of them show short emissive wavelengths with primary emission bands below 630 nm. With the advances in optical techniques for detecting and imaging, polymeric gel materials with low-energy near-infrared (NIR) luminescence (650 ~ 900 nm) are more preferred owing to less interference from background

* Corresponding authors.
E-mail addresses: weipeng@nbu.edu.cn (P. Wei), shenjw1184@126.com (J. Shen), luwei@nimte.ac.cn (W. Lu).
[1] Shuhui An and Xiaoyi Zhang contributed equally to this work.

https://doi.org/10.1016/j.cej.2023.142307
Received 18 December 2022; Received in revised form 10 February 2023; Accepted 4 March 2023
Available online 9 March 2023

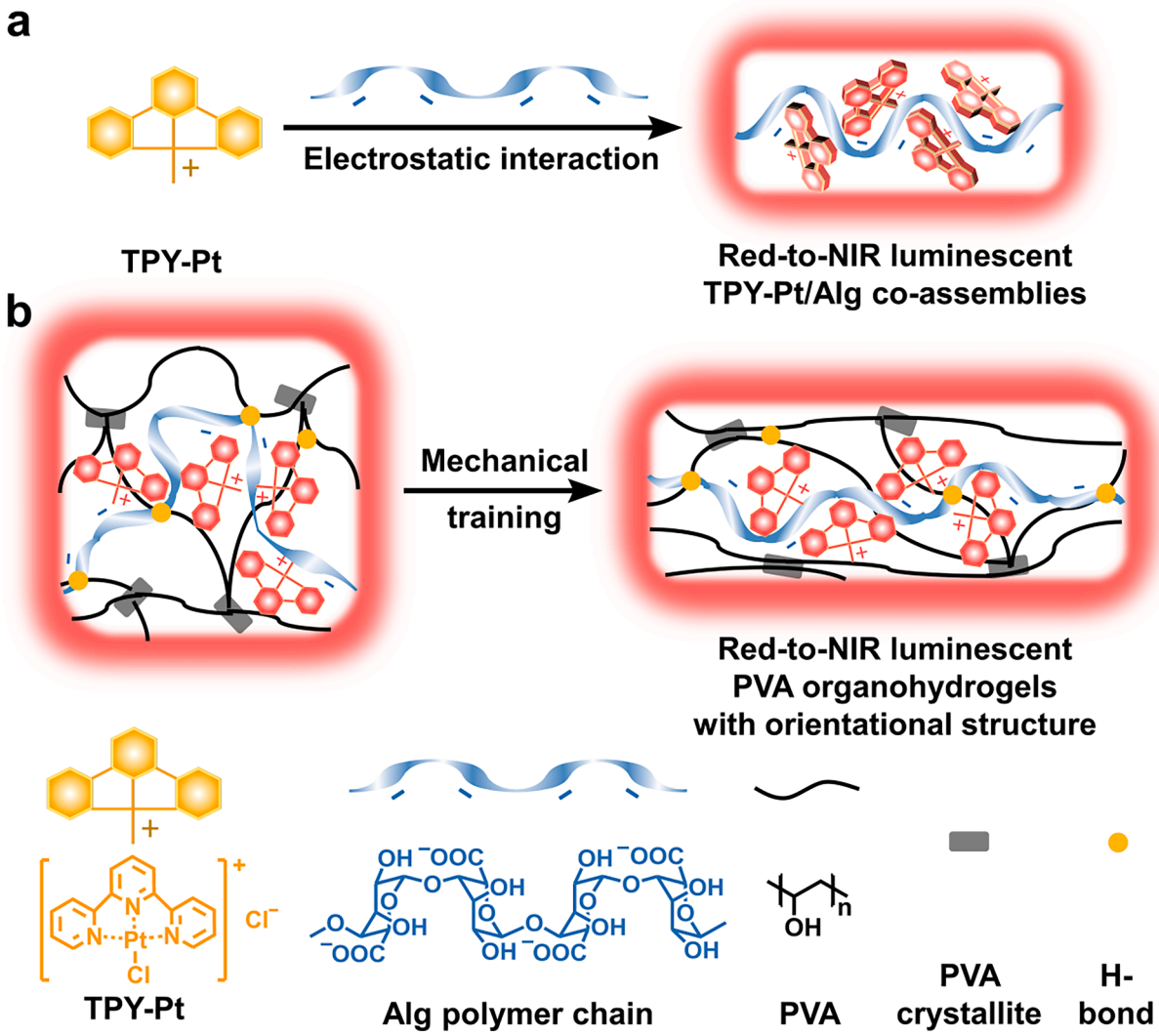

Scheme 1. Schematic illustration indicating the construction of red-to-NIR luminescent supramolecular TPY-Pt/Alg co-assemblies and PVA organohydrogels. (a) AIE-active TPY-Pt luminogens were positively charged and spontaneously self-assembled with Alg polymer *via* electrostatic interactions to form red-to-NIR luminescent TPY-Pt/Alg co-assemblies. (b) Physical incorporation of TPY-Pt/Alg co-assemblies into crosslinked PVA networks led to red-to-NIR luminescent organohydrogels whose mechanical strength could be largely enhanced by mechanical training to induce the formation of anisotropic structures.

auto-fluorescence, less light scattering and minimized absorption by environment water [25–27]. However, despite many advances in red-to-NIR luminogens [28,29], such red-to-NIR luminescent polymeric gels are still quite few [30–32] primarily owing to the difficulties of synthesis. Specifically, although nearly all red-to-NIR luminogens can be physically incorporated into crosslinked polymer matrix to produce the corresponding gels, these luminescent molecules usually have large conjugated structure and are thus prone to form π-π stacked aggregates, which may not only affect their luminescence properties, but also cause varying and heterogeneous distribution of these luminogens in the gels. Chemical copolymerization is a good approach to ensure the composition and luminescence stability of red-to-NIR luminescent gels, but usually requires multistep organic synthetic procedures to introduce additional polymerizable groups into the red-to-NIR luminogens. It significantly raises the difficulties to obtain red-to-NIR luminescent gels and thus largely restricts their intensive studies, especially for the researchers with material science or biological backgrounds, who are usually not familiar with organic synthesis.

Supramolecular assembly of common luminogens may be a more promising and easier solution to prepare red-to-NIR luminescent gels. As is well known, the luminescent dyes are usually brought into close proximity in supramolecular assemblies and thus favorable for coupling of these dyes' transition dipole moments [33], possibly leading to remarkable red shift in emission to long-wavelength or even the NIR range. For example, Wu et al. [34,35] recently copolymerized the hydrophobic 4′-(N-vinyl benzyl-4-pyridinyl)-2,2′:6′,2′'-terpyridine perchlorate (VPTP) chromophore with short unimer emission band (~450 nm) into hydrophilic polymer networks to produce a series of polymeric gels with low-energy dimer emission band (~570 nm). Although emission of such gels still falls far from the NIR range, the observed large red-shift emission of supramolecular VPTP assemblies is highly inspiring. Furthermore, if the luminogens with aggregation-induced emission (AIE) characteristics were employed to form supramolecular assemblies in polymeric gels [36,37], significantly enhanced and red-shifted luminescence would be guaranteed because of the close aggregation of these AIE-active molecules in polymer networks. Despite the great potential of this supramolecular assembly strategy, it is still a challenging task to develop robust AIE-active polymeric gels with the preferred red-to-NIR emission. In addition, other features such as self-healing, remolding and especially mechanical toughness, are also expected for enhancing the functions of such red-to-NIR luminescent gels.

Herein, we propose to utilize polymer-induced supramolecular assembly of AIE-active (2,2′:6′,2′'-terpyridine) platinum(II) chloride (TPY-Pt) luminogen to develop a robust type of red-to-NIR luminescent

polymeric organohydrogels. As illustrated in Scheme 1a, the TPY-Pt luminogen is positively charged and thus readily soluble in water. It is nearly non-luminescent in aqueous solution, but emits intense orange luminescence with a broad emission band around 595 nm when self-aggregated in poor solvent, indicating its typical AIE nature. Upon addition of the negatively charged alginate (Alg) polymer into TPY-Pt aqueous solution, the intra-molecular motions of TPY-Pt are largely restricted owing to its electrostatic interaction with the carboxyl groups of Alg chain, resulting in turn-on luminescence response. The close proximity of these TPY-Pt dyes around Alg polymer chain is favorable for the coupling of the dyes' transition dipole moments, resulting in an unexpectedly large red shift in emission (~93 nm) to the red-to-NIR range (Scheme 1a). Interestingly, such intense red-shifted emission is capable of being finely retained in crosslinked poly(vinyl alcohol) (PVA) networks and even can be reversibly regulated by pH variation. Owing to their totally physical crosslinking nature, the obtained organohydrogels also have satisfying self-healing and remolding capacities. After being subject to mechanical training [38], mechanically tough and red-to-NIR luminescent PVA organohydrogels with biocompatibility were produced (Scheme 1b). Such multi-functional red-to-NIR luminescent organohydrogels are expected to find wide application potentials in fields of luminescence imaging, sensing, secure information display and encryption.

2. Experimental section

2.1. Materials

Potassium tetrachloroplatinate (K_2PtCl_4, 98%), 2,2′:6′,2″-terpyridine (98%), 1799 poly(vinyl alcohol) (1799 PVA, M_w = 44.05, alcoholysis degree = 98 ~ 99%), dimethyl sulfoxide (DMSO, >99%), ethylene glycol (EG, >99%), ethyl acetate (99%), sodium hydroxide (NaOH, 97%) and anhydrous sodium acetate (reagent grade) were provided by Aladdin Biochemistry Co., Ltd. Sodium alginate (Alg, ≥99.5%) and hydrochloric acid (HCl, 36 ~ 38%) were commercially provided by Sinopharm Chemical Reagent Co., Ltd.

2.2. Synthesis and characterization of (2,2′:6′,2′′-terpyridine) platinum (II) chloride complex (TPY-Pt)

Potassium tetrachloroplatinate (0.372 g, 0.9 mmol) was dissolved in 7 mL of deionized water, and then 400 μL DMSO and 2,2′:6′,2″-terpyridine (0.208 g, 0.9 mmol) were added successively. The mixture was stirred at 110 °C (refluxing condition) for about 3 h until the red mixture became clear. The clear solution was cooled down to room temperature and acidified with four drops of concentrated HCl solution. Then it was left overnight for total precipitation of product. After being filtered, washed by ethyl acetate and finally dried under vaccum, the orange solid was obtained in 90% yield (0.4 g).

2.3. Preparation of red-to-NIR luminescent organohydrogels

After totally dissolving PVA in mixed deionized water and EG at 100 °C, aqueous Alg solution and EG solution of TPY-Pt were successively added and thoroughly mixed respectively. Then, stirring was stopped to remove air bubbles in the mixture. Subsequently, the mixture was cast into self-made molds and cooled down to room temperature. Finally, the above system was left in refrigerator at −20 °C for 20 min to produce red-to-NIR luminescent organohydrogels. The organohydrogels used in this work were prepared with PVA concentration of 108.37 mg/mL, TPY-Pt concentration of 0.2515 mg/mL (cationic concentration with 0.5 mM) and Alg concentration of 0.15 mg/mL (carboxylate radical concentration with 0.75 mM). The volume ratio of EG and water was 3:2.

2.4. Preparation of patterned red-to-NIR luminescent organohydrogels

Paper stamps were produced by completely soaking patterned filter paper in 1 M HCl solution, which were taken out and dried in a 60 °C oven. They were placed on red-to-NIR luminescent organohydrogels with dry surface for 3 min to avoid pattern from being smudged, during which pressure was applied to make the pattern printed evenly.

2.5. Investigation into self-healing property of red-to-NIR luminescent organohydrogels

The original red-to-NIR luminescent organohydrogel samples with different shapes were cut into several pieces. In the self-healing experiments, the separated gel surfaces were re-contacted and a drop of solution (volume ration of EG and water = 3:2) was added on the cut. The joint was heated at 90 °C under pressure for 2 h and then cooled down to room temperature.

2.6. Investigation into remolding property of red-to-NIR luminescent organohydrogels

The organohydrogel pieces were first melted at 100 °C, and then poured into new molds. After being cooled at −20 °C for 20 min, red-to-NIR luminescent organohydrogels with different shapes were remolded. This process could be repeated for at least 5 times.

2.7. Preparation of anisotropic red-to-NIR luminescent organohydrogels

The as-prepared red-to-NIR luminescent organohydrogels were stretched to 2.3 times of original length at a speed of 1000 mm/min, held for 30 s and then unloaded. Such mechanical training process was repeated for 20, 50, 100 or 300 times.

2.8. Characterization

^{1}H NMR spectrum of TPY-Pt was measured on Bruker Advance AMX spectrometer at 400 MHz in D_2O. ESI mass spectrum of TPY-Pt was recorded on a mass spectrometer (AB Sciex, 4600). Emission spectra, luminescence decay curve and average lifetime were recorded by a spectrofluorometer (HORIBA, FL3-111) equipped with a xenon (Xe) lamp (450 W). Internal quantum efficiencies of the solid TPY-Pt powder and red-to-NIR luminescent PVA gels were measured using an integrating sphere apparatus by the absolute method on a quantum efficiency tester (Otsuka Photal Electronics, QE-2100), and the wavelength range of signal reception was from 510 nm to 850 nm. UV–Vis absorption spectra were recorded on a spectrophotometer (Perkin-Elmer, Lambda 950). TEM images were acquired by a transmission electron microscope (JEOL2100, JEM2100). Dynamic light scattering and zeta potential were carried out at Malvern Zetasizer Nano ZS. Confocal images of organohydrogels in wet state were obtained by a confocal laser microscope (LEICA, TCS SPS) and the data were collected from 415 nm to 705 nm. Images showing self-healing process were taken by a polarizing microscope (OLYMPUS, BX51). Rheological property of organohydrogels was characterized by a rotational rheometer (TA, HR-3). SEM images were acquired by a scanning electron microscope (Hitachi, S4800). Mechanical training and mechanical tests of NIR luminescent organohydrogels were carried out on a universal testing machine (Zwick/Roell Z1.0). All digital photos were taken by a Sony camera (IMX 315) on iPhone 7.

3. Results

3.1. Red-to-NIR luminescent supramolecular TPY-Pt/Alg co-assemblies

TPY-Pt was designed as a cationic luminogen by coordinating Pt^{2+} with terpyridine (TPY) and one Cl^- ion (Fig. S1) [39]. Its chemical

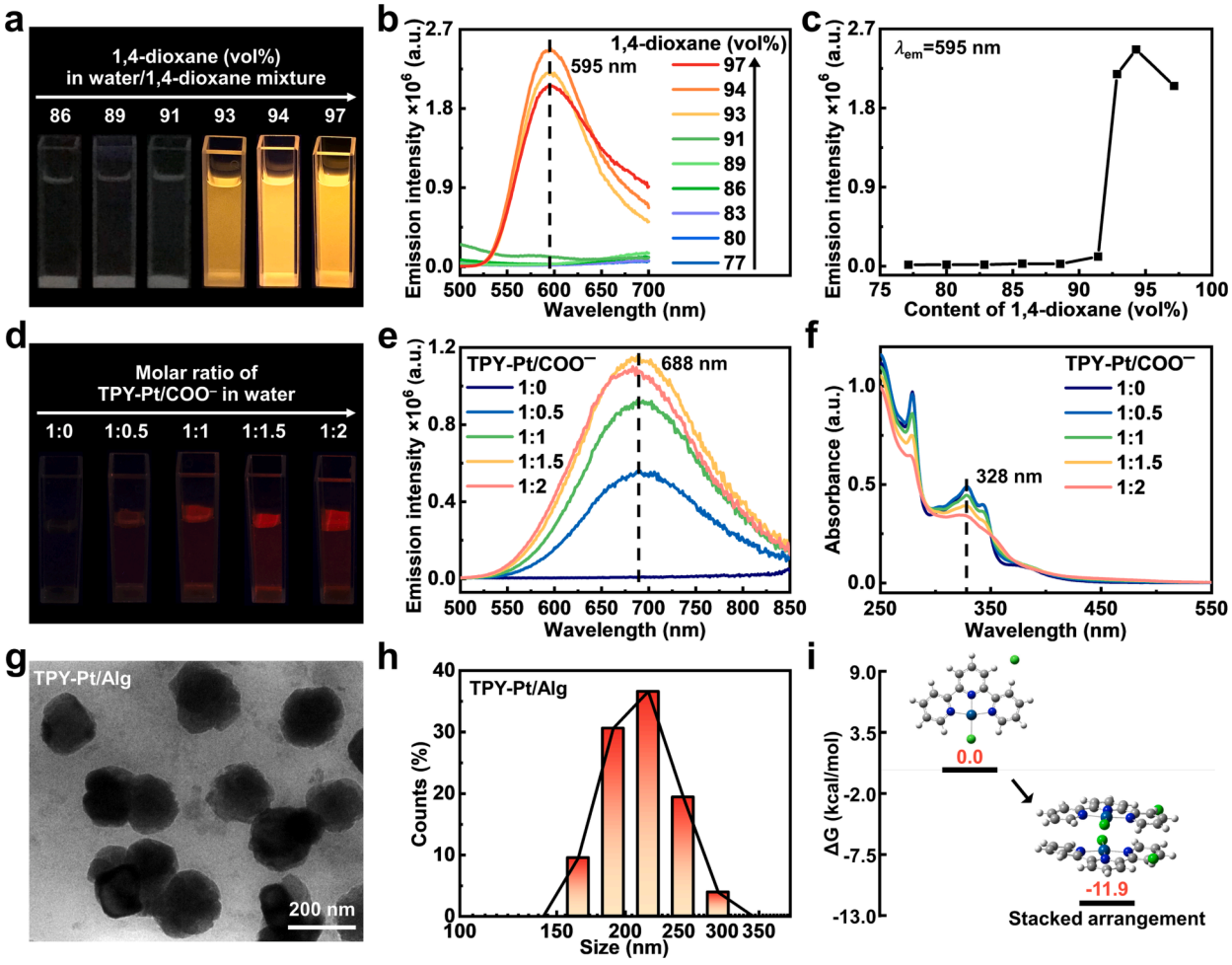

Fig. 1. Luminescent properties of the TPY-Pt luminogen and supramolecular TPY-Pt/Alg co-assemblies. (a) Photos of TPY-Pt (0.047 mM) in the water/1,4-dioxane mixtures, (b) their emission spectra (λ_{ex} = 365 nm) and (c) emission intensities at 595 nm as a function of the volume content of 1,4-dioxane. (d) Photos of TPY-Pt aqueous solution (0.05 mM) with increasing concentration of COO^- in Alg polymer, and the corresponding (e) emission spectra (λ_{ex} = 365 nm) and (f) UV–Vis spectra. (g) TEM image and (h) size distribution of the TPY-Pt/Alg co-assemblies in aqueous suspension with 0.01 mM TPY-Pt and 0.015 mM COO^- in Alg polymer. (i) Relative Gibbs free energies, ΔG, of TPY-Pt in the form of stacked arrangement. All luminescent photos were taken under a 365 nm UV lamp (8 W).

structure was clearly confirmed by proton (^{1}H) nuclear magnetic resonance (NMR), electro spray ionization-mass spectroscopy (ESI-MS) (Fig. S2 ~ S3). Solid TPY-Pt luminogen emits at around 630 nm with the internal quantum efficiency of 11.53% and average luminescence lifetime of 707.4 ns (Fig. S4 ~ S5). The positively charged TPY-Pt is readily soluble in deionized water, but insoluble in 1,4-dioxane (Fig. S6). Under 365 nm UV light, it is nearly non-luminescent in water or water/1,4-dioxane mixtures, but begins to emit orange light around 595 nm when the content of 1,4-dioxane is above 93 vol% (Fig. 1a-c). With increasing 1,4-dioxane content to induce more TPY-Pt aggregates, the orange emission intensity rapidly rises and reaches the maximum in 94 vol% 1,4-dioxane solution. But when the 1,4-dioxane content reaches 97 vol%, the TPY-Pt aggregates will be large enough to form precipitations in the bottom of cuvette (Fig. S6), resulting in decreasing intensity of the suspension. These results clearly indicate the AIE nature of the designed TPY-Pt luminogen. No obvious luminescence is observed in aqueous solution of TPY-Pt because the excited state of luminogen is rapidly quenched by solvent or oxygen through non-radiative deactivation [40], while the bright emission appears in the aggregation states due to the largely reduced exposure to solvent and oxygen [41].

The AIE-active and cationic characteristics of TPY-Pt molecules further encouraged us to explore their aggregation along negatively charged Alg polymer chain for developing highly luminescent supramolecular TPY-Pt/Alg co-assemblies. As a comparison, addition of negatively charged small-molecule sodium acetate into the TPY-Pt solution still exhibited no obvious emission (Fig. S7). Unexpectedly, red-to-NIR luminescence, rather than the expected orange emission, was immediately observed upon the addition of Alg into aqueous TPY-Pt solution (Fig. 1d), as evidenced by appearance of new red-to-NIR emission band around 688 nm (Fig. 1e). Compared with the AIE emission band that was expected to appear around 595 nm, a red-shifted emission as large as 93 nm was observed. As shown in Fig. 1e, with increasing Alg concentration, this new red-to-NIR emission band gradually increased and reached the plateau when the molar ratio of negative carboxyl groups in Alg was above 1.5 times that of TPY-Pt. This was because increasing Alg amount would result in the formation of more supramolecular TPY-Pt/Alg co-assemblies through electrostatic interactions. But when the content of Alg was too high (i.e., the molar ratio of negative carboxyl groups in Alg was above 2 times that of TPY-Pt), the supramolecular TPY-Pt/Alg co-assemblies may decompose, resulting in the reduction of emission intensity at 688 nm. Meanwhile, the UV–Vis titration spectra revealed noticeable decrease of the absorption peak of TPY-Pt at 328 nm and slight increase of the shoulder peak above 350 nm (Fig. 1f). Additionally, an obvious Tyndall effect was observed for the TPY-Pt/Alg suspension (Fig. S8). All these results suggested the formation of supramolecular TPY-Pt/Alg co-assemblies. Direct evidences for the co-assemblies came from TEM image (Fig. 1g) and dynamic light scattering result (Fig. 1h), which demonstrated the formation of quasi-

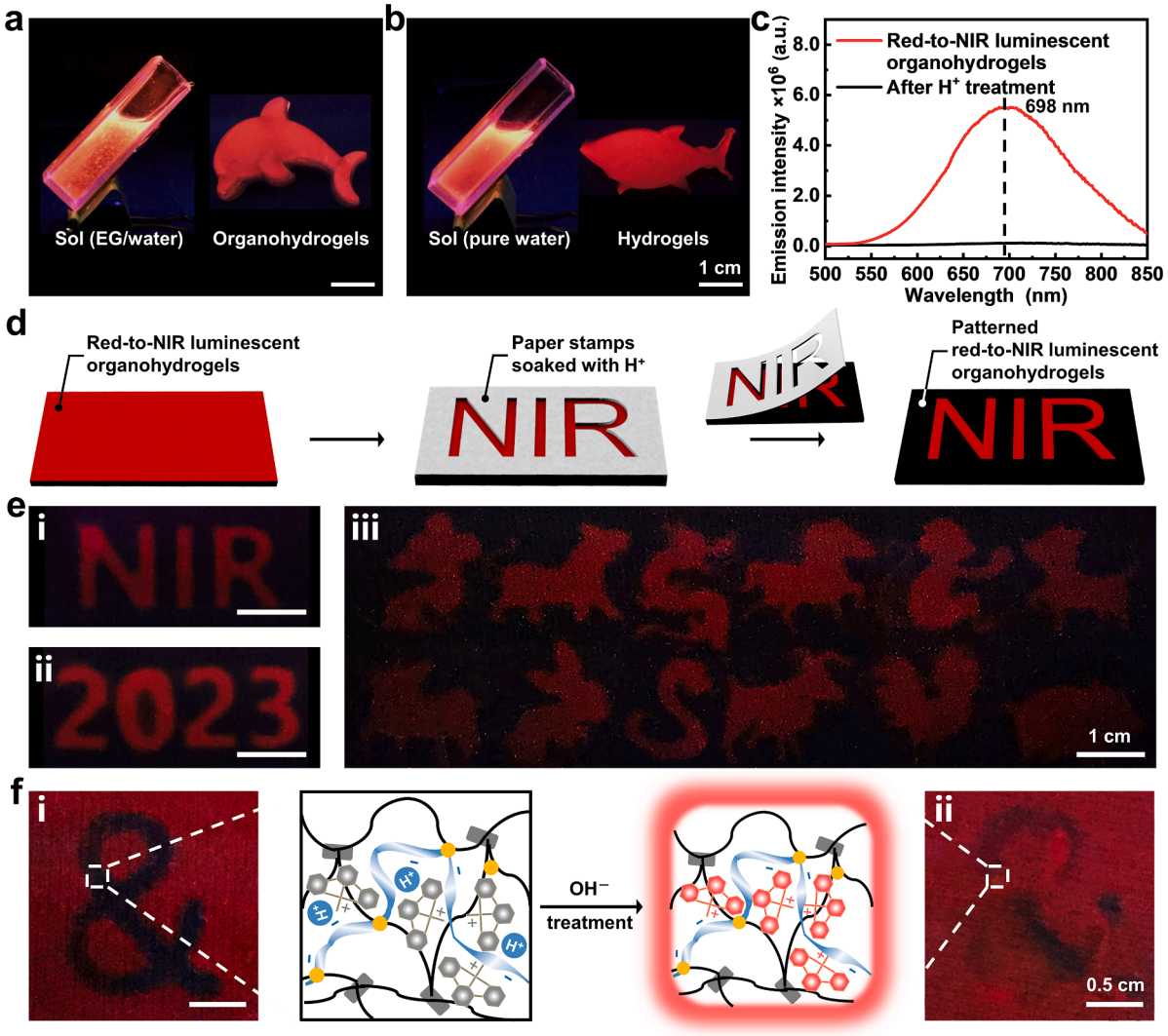

Fig. 2. Construction of red-to-NIR luminescent PVA organohydrogels and their pH-triggered red-to-NIR luminescence response. (a-b) Photos of the prepared red-to-NIR luminescent suspensions and gels (thickness: 7 mm). (c) Emission spectra of the obtained organohydrogels before and after being treated by paper stamps soaked with 1 M HCl. (d) Schematic illustration of method for pattern printing. (e) Photos of several patterned red-to-NIR emissive organohydrogels (thickness: 0.3 mm) with information of different types and complexity. (f) Photos and proposed mechanism of red-to-NIR emissive organohydrogels (thickness: 0.3 mm) successively treated by paper stamps soaked in H^+ and OH^- solutions with equal 0.05 M concentration. All photos were taken under a 365 nm UV lamp (8 W). (For interpretation of the references to colour in this figure legend, the reader is referred to the web version of this article.)

sphere TPY-Pt/Alg assemblies with average size of ~ 200 nm in suspension. Zeta potential of the suspension was −7.6 mV (Fig. S9), indicating excess anions on the surface of TPY-Pt/Alg assemblies. Also, density functional theory calculation results suggested that the stacked arrangement of TPY-Pt luminogens had relatively lower Gibbs free energy (Table. S1, Fig. 1i, S10 and S11). On the basis of these results, it was reasoned that the red-shifted emission band around 688 nm derived from the coupling of the dyes' transition dipole moments in the supramolecular TPY-Pt/Alg co-assemblies [33].

3.2. Red-to-NIR luminescent PVA organohydrogels

The intense red-to-NIR emission of supramolecular TPY-Pt/Alg co-assemblies further encouraged us to develop the rarely reported red-to-NIR luminescent polymeric organohydrogels or hydrogels. As a proof-of-concept, PVA was herein chosen as the gel matrix because it was uncharged and expected to have little influence on the stability of TPY-Pt/Alg co-assemblies. In a typical example, the PVA powder was firstly dissolved in mixtures of ethylene glycol and water at 100 °C, and was uniformly mixed with suspension of TPY-Pt/Alg co-assemblies. The mixture was then poured into the self-made mold and frozen at −20 °C for 20 min to induce the physical crosslinking between PVA polymer chains *via* crystalline domains and hydrogen bonds. During the freezing process, there formed strong hydrogen bonds and intermolecular interaction between the PVA and Alg molecular chains [42], making the luminescent TPY-Pt/Alg co-assemblies evenly and stably distributed in the organohydrogel matrix (Fig. S12). As a result, the red-to-NIR luminescence of supramolecular TPY-Pt/Alg co-assemblies was not only well-retained in the PVA organohydrogels, but also further red-shifted to show an intense red-to-NIR emission band centered at 698 nm (Fig. 2a, 2c, S13a and S14) with internal quantum efficiency of 2.84%. When physically incoporating TPY-Pt/Alg co-assemblies into aqueous PVA solution and then subjecting them to five freezing/thawing cycles, red-to-NIR luminescent PVA hydrogels were obtained with a primary emission band centered at 708 nm (Fig. 2b, S13b and S15) with internal quantum efficiency of 1.63%. Note that the preparation of red-to-NIR luminescent PVA organohydrogels is much easier than that of PVA hydrogels, because EG has smaller chemical polarity than H_2O and thus is capable of forming vast hydrogen-bonding interactions between PVA chains, which facilitates the formation of PVA crystalline domains

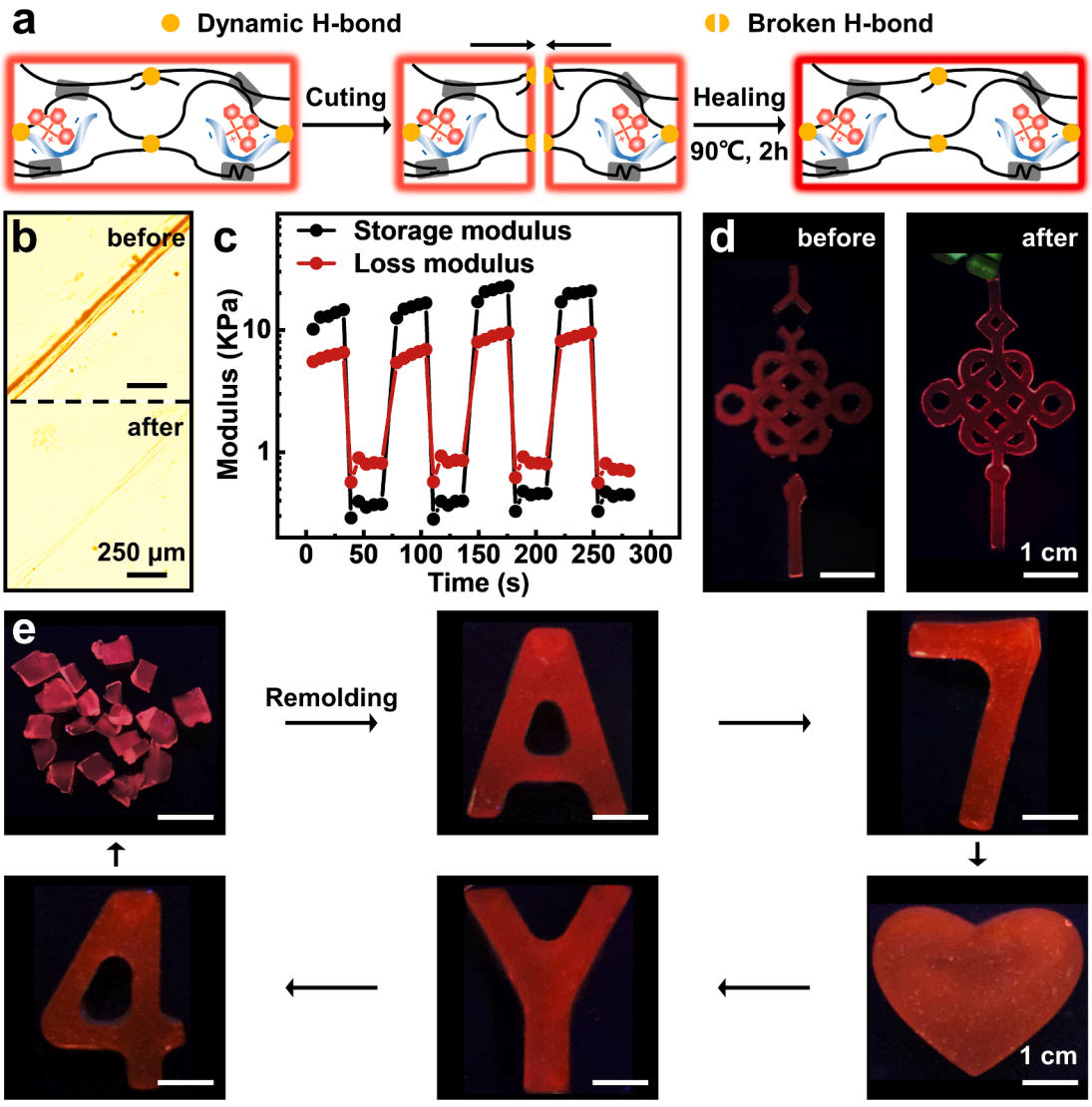

Fig. 3. Self-healing and remolding properties of the red-to-NIR luminescent PVA organohydrogels. (a) Proposed self-healing mechanism of the PVA organohydrogels. (b) Microscopic images of the cut before and after self-healing process. (c) Rheological properties of the PVA organohydrogels under alternating strain of 1% and 300% at a constant frequency of 1 Hz and temperature of 90 °C. (d) Photos showing that several organohydrogel slices (thickness: 2 mm) could be healed together to form integrated object which can be lifted up. (e) Photos showing that organohydrogel pieces could be remolded as distinct intact gel structures after being heated at 100 °C for a short time (e.g., 2 min) and reshaped at −20 °C for 20 min in the pre-designed molds (thickness: 7 mm). All luminescent photos were taken under a 365 nm UV lamp (8 W). (For interpretation of the references to colour in this figure legend, the reader is referred to the web version of this article.)

through one simple freezing step instead of repeated freezing/thawing cycles [43]. Compared with suspension of TPY-Pt/Alg co-assemblies, both the normalized UV–Vis absorption bands (Fig. S16) and NIR emission bands of the gels exhibited gently bathochromic shifts, leading one to speculate the formation of more compact TPY-Pt/Alg co-assembly structures in gel networks caused by stronger coupling of the dyes' transition dipole moments [33].

Since the red-to-NIR luminescence of PVA organohydrogels was derived from the supramolecular TPY-Pt/Alg co-assemblies stabilized by the electrostatic interaction between cationic TPY-Pt luminogens and anionic Alg polymer, it was possible to modulate the red-to-NIR luminescence by utilizing H^+ to acidify Alg polymer that decomposed the supramolecular TPY-Pt/Alg co-assemblies. To prove this, the paper stamps soaked with 1 M HCl was carefully placed on the PVA organohydrogels for 3 min, during which time H^+ had diffused into the gel matrix to tranform anionic Alg polymer to protonated alginic acid, significantly reducing the intensity of red-to-NIR emission (Fig. 2d). This observation was consistent with the recorded emission spectra, which showed the disappearance of red-to-NIR emission band around 698 nm (Fig. 2c). On the basis of this pH-triggered red-to-NIR luminescence response, various luminescent patterns could be easily created on the PVA organohydrogels, including English letters "NIR" (Fig. 2e-i), Arabic numbers "2023" (Fig. 2e-ii), Chinese character "福" (blessing) and the rose painting (Fig. S17). In view of its operational simplicity, more complex red-to-NIR luminescent patterns with the twelve Chinese zodiac signs were further readily printed by the ion-printing method (Fig. 2e-iii). For demonstrating the reversibility of red-to-NIR luminescence response, HCl-printed luminescence quenching parts of the PVA organohydrogels were re-printed by the paper stamp containing equivalent amount of NaOH. As depicted in Fig. 2f, the luminescence was quickly recovered. Besides, the luminescence response processes after acid/base treatments can be repeated (Fig. S18). These results expanded the possibility to produce red-to-NIR luminescent patterns on gel systems, holding great potential for biological sensing or information decryption uses.

Other significant characteristics of the red-to-NIR luminescent PVA organohydrogels included the self-healing and remolding properties owing to their completely supramolecular crosslinking interactions

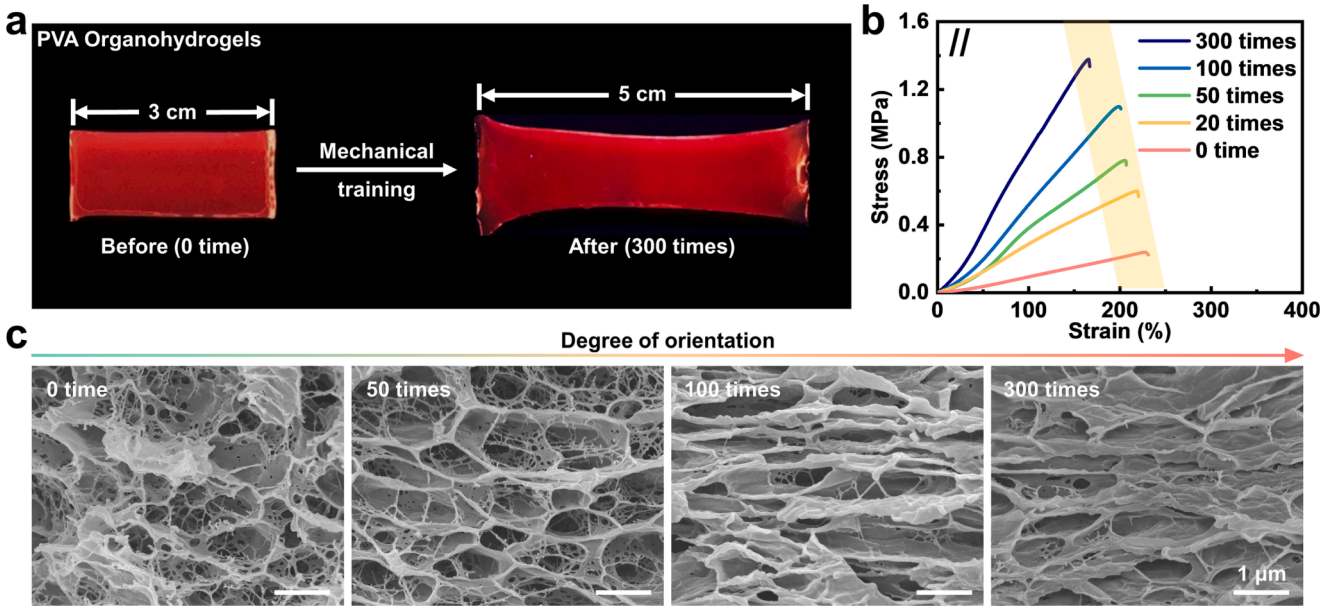

Fig. 4. Anisotropic and tough PVA organohydrogels with red-to-NIR emission. (a) Photos of one PVA organohydrogel sheet before (thickness: 2 mm) and after (thickness: 1 mm) 300-time mechanical training (prestretching). (b) Tensile stress–strain curves of the PVA organohydrogel samples after prestretching for different times (the tensile direction is parallel to the direction of orientation). (c) SEM images of the freeze-dried PVA organohydrogel samples after prestretching for different times. All luminescent photos were taken under a 365 nm UV lamp (8 W). (For interpretation of the references to colour in this figure legend, the reader is referred to the web version of this article.)

(Fig. 3a). The optical images in Fig. 3b showed that the cut between two organohydrogel blocks would disappear after being heated at 90 °C for 2 h, demonstrating its self-healing capability. Rheological tests were further examined by applying alternating strain of 1% and 300% at a constant frequency of 1 Hz and temperature of 90 °C. At higher 300% strain, loss modulus (G″) was larger than storage modulus (G′), indicating liquid-like behavior of organohydrogels caused by the disruption of dynamic crosslinking networks. At lower 1% strain, G′ was larger than G″ and both of them recovered nearly to the original values, suggesting the gel-like behavior due to the reconstruction of supramolecular networks (Fig. 3c). On this basis, it was demonstrated that several organohydrogel slices could be fully self-healed together to form different-shaped integrated objects such as Chinese knot (Fig. 3d), auspicious cloud and lantern (Fig. S19). Furthermore, the red-to-NIR luminescent organohydrogels also exhibited superb thermoplasticity. Organohydrogel pieces were able to be remolded as distinct intact gel structures after being heated at 100 °C for a short time (e.g., 2 min) and reshaped at −20 °C for 20 min in the pre-designed molds (Fig. 3e and S20). Interestingly, such remolding process could be repeated for many times without affecting the intense red-to-NIR luminescence of the organohydrogels. These results indicate that our organohydrogels could be self-healed and remolded into different shapes.

3.3. Anisotropic PVA organohydrogels with red-to-NIR emission

Owing to the presence of dual crosslinking structures *via* crystalline domains and hydrogen bonds, the as-prepared red-to-NIR luminescent organohydrogels with solvent content ~ 90% could bear a moderate stress of 0.2 MPa (Fig. 4b), which was still far inferior to that of skeletal muscles (~1 MPa) [44]. Biological studies revealed that tough strength of natural muscles is largely attributed to the aligned nanofibrils structures, which have seldomly been reproduced in synthetic gels. Inspired by this finding, we further proposed a mechanical training strategy (Sch. S1) to induce anisotropic orientational structures in the crosslinked PVA polymer networks. To this end, the as-prepared red-to-NIR luminescent organohydrogels were subject to repeated prestretching for hundred times (Fig. 4a, S21 and S22). SEM images of the prestretched organohydrogels shown in Fig. 4c and S23 indicated that the crosslinked polymer networks indeed became anisotropic and formed orientation structures along the prestretching direction. Note that, although the polymer networks mostly recovered to the initial random distribution elastically after each prestretching experiment, repeated prestretching for a large number of times will accumulate enough plastic deformation to elongate and preserve the polymer networks along the prestretching direction. Consequently, the orientation structure was increasingly evident with more prestretching times (from 50 to 300 times). Accordingly, mechanical strength of the organohydrogels was gradually enhanced with increasing prestretching times and was able to bear a high stress of 1.4 MPa after 300-time prestretching operations (Fig. 4b, S24 and S25). Besides, biocompatibility of the as-prepared red-to-NIR luminescent gels had been demonstrated (Fig. S26 and S27).

4. Conclusions

We have reported a robust type of AIE-active supramolecular TPY-Pt/Alg co-assemblies with intense red-to-NIR luminescence, followed by their physical incorporation into crosslinked PVA polymer networks to produce red-to-NIR luminescent polymeric organohydrogels. The supramolecular TPY-Pt/Alg co-assemblies were prepared from the self-assembly of cationic TPY-Pt luminogens and anionic Alg polymer *via* electrostatic interactions. Owing to the coupling of the dyes' transition dipole moments, unexpected and large red emission shift (~93 nm) was observed for the TPY-Pt/Alg aggregates. Importantly, such red-to-NIR emission could be well-preserved and further enhanced after physically introducing TPY-Pt/Alg co-assemblies into PVA organohydrogels and hydrogels. Additionally, the developed red-to-NIR luminescent organohydrogels had good self-healing and remolding abilities. Upon further mechanical training, mechanically tough PVA organohydrogels with intense red-to-NIR luminescence and biocompatibility were obtained, suggesting their possibility to be processed into arbitrary-shaped materials suitable for wide potential bio-related uses. Moreover, considering the facile preparation of the present system and its modular design principle, the proposed strategy is expected to be generally applicable for many other luminogens and potentially inspire the future

development of numerous NIR luminescent materials.

Declaration of Competing Interest

The authors declare that they have no known competing financial interests or personal relationships that could have appeared to influence the work reported in this paper.

Data availability

Data will be made available on request.

Acknowledgments

We gratefully acknowledge the Zhejiang Provincial Natural Science Foundation of China (LD22A020002), the Youth Innovation Promotion Association of Chinese Academy of Sciences (2019297), the K. C. Wong Education Foundation (GJTD-2019-13), the Basic Technology Research Program of Zhejiang Province (BY23H180015), the Natural Science Foundation of Ningbo City (2017A610183), the Foundation of Ningbo Science and Technology Bureau (202002N3182) and the Medical Health Science and Technology Project of Zhejiang Provincial Health Commission (2020KY825). The authors thank Shuangshuang Wu, Hui Shang, Baoyi Wu, Guangqiang Yin, Shuxin Wei for help with experiments and technical discussions.

Appendix A. Supplementary data

Supplementary data to this article can be found online at https://doi.org/10.1016/j.cej.2023.142307.

References

[1] H. Wang, X. Ji, Z. Li, F. Huang, Fluorescent supramolecular polymeric materials, Adv. Mater. 29 (2017) 1606117, https://doi.org/10.1002/adma.201606117.
[2] S. Wei, Z. Li, W. Lu, H. Liu, J. Zhang, T. Chen, B. Tang, Multicolor fluorescent polymeric hydrogels, Angew. Chem. Int. Ed. 60 (2021) 8608, https://doi.org/10.1002/anie.202007506.
[3] Y. Li, D.J. Young, X.J. Loh, Fluorescent gels: a review of synthesis, properties, applications and challenges, Mater. Chem. Front. 3 (2019) 1489, https://doi.org/10.1039/c9qm00127a.
[4] W. Lu, S. Wei, H. Shi, X. Le, G. Yin, T. Chen, Progress in aggregation-induced emission-active fluorescent polymeric hydrogels, Aggregate 2 (2021) e37.
[5] Y. Zhao, C. Shi, X. Yang, B. Shen, Y. Sun, Y. Chen, X. Xu, H. Sun, K. Yu, B. Yang, Q. Lin, Ph- and temperature-sensitive hydrogel nanoparticles with dual photoluminescence for bioprobes, ACS Nano 10 (2016) 5856, https://doi.org/10.1021/acsnano.6b00770.
[6] K. Benson, A. Ghimire, A. Pattammattel, C.V. Kumar, Protein biophosphors: biodegradable, multifunctional, protein-based hydrogel for white emission, sensing, and pH detection, Adv. Funct. Mater. 27 (2017) 1702955, https://doi.org/10.1002/adfm.201702955.
[7] G. Weng, S. Thanneeru, J. He, Dynamic coordination of Eu-iminodiacetate to control fluorochromic response of polymer hydrogels to multistimuli, Adv. Mater. 30 (2018) 1706526, https://doi.org/10.1002/adma.201706526.
[8] N. Mehwish, X. Dou, Y. Zhao, C.L. Feng, Supramolecular fluorescent hydrogelators as bio-imaging probes, Mater. Horiz. 6 (2019) 14, https://doi.org/10.1039/c8mh01130c.
[9] G. Lin, M. Si, L. Wang, S. Wei, W. Lu, H. Liu, Y. Zhang, D. Li, T. Chen, Dual-Channel Flexible Strain Sensors Based on Mechanofluorescent and Conductive Hydrogel Laminates, Adv. Optical Mater. 10 (2022) 2102306, https://doi.org/10.1002/adom.202102306.
[10] S. Wu, H. Shi, W. Lu, S. Wei, H. Shang, H. Liu, M. Si, X. Le, G. Yin, P. Theato, T. Chen, Aggregation-induced emissive carbon dots gels for octopus-inspired shape/color synergistically adjustable actuators, Angew. Chem. Int. Ed. 60 (2021) 21890, https://doi.org/10.1002/anie.202107281.
[11] D. Lu, M. Zhu, S. Wu, Q. Lian, W. Wang, D. Adlam, J.A. Hoyland, B.R. Saunders, Programmed multiresponsive hydrogel assemblies with light-tunable mechanical properties, actuation, and fluorescence, Adv. Funct. Mater. 30 (2020) 1909359, https://doi.org/10.1002/adfm.201909359.
[12] Y. Lin, C. Li, G. Song, C. He, Y.Q. Dong, H. Wang, Freezing-induced multi-colour emissions of AIE luminogen di(4-propoxyphenyl) dibenzofulvene, J. Mater. Chem. C 3 (2015) 2677, https://doi.org/10.1039/c4tc02805h.
[13] R. Merindol, G. Delechiave, L. Heinen, L.H. Catalani, A. Walther, Modular design of programmable mechanofluorescent DNA hydrogels, Nat. Commun. 10 (2019) 528, https://doi.org/10.1038/s41467-019-08428-2.
[14] X. Liu, B. Li, W. Wang, Y. Zhang, H. Li, Z. Li, Multistimuli-responsive hydrogels with both anisotropic mechanical performance and anisotropic luminescent behavior, Chem. Eng. J. 449 (2022), 137718, https://doi.org/10.1016/j.cej.2022.137718.
[15] Z. Li, G. Wang, Y. Wang, H. Li, Reversible phase transition of robust luminescent hybrid hydrogels, Angew. Chem. Int. Ed. 57 (2018) 2194, https://doi.org/10.1002/anie.201712670.
[16] J. Wang, S. Sun, B. Wu, L. Hou, P. Ding, X. Guo, M.A. Cohen Stuart, J. Wang, Processable and luminescent supramolecular hydrogels from complex coacervation of polycations with lanthanide coordination polyanions, Macromolecules 52 (2019) 8643, https://doi.org/10.1021/acs.macromol.9b01568.
[17] M.D. Weber, L. Niklaus, M. Proschel, P.B. Coto, U. Sonnewald, R.D. Costa, Bioinspired hybrid white light-emitting diodes, Adv. Mater. 27 (2015) 5493, https://doi.org/10.1002/adma.201502349.
[18] A. Cayuela, S.R. Kennedy, M.L. Soriano, C.D. Jones, M. Valcarcel, J.W. Steed, Fluorescent carbon dot-molecular salt hydrogels, Chem. Sci. 6 (2015) 6139, https://doi.org/10.1039/c5sc01859e.
[19] X.-Y. Du, C.-F. Wang, G. Wu, S.u. Chen, The rapid and large-scale production of carbon quantum dots and their integration with polymers, Angew. Chem. Int. Ed. 60 (16) (2021) 8585–8595.
[20] X. Ji, R.T. Wu, L. Long, X.S. Ke, C. Guo, Y.J. Ghang, Encoding, reading, and transforming information using multifluorescent supramolecular polymeric hydrogels, Adv. Mater. 30 (2018) 1705480, https://doi.org/10.1002/adma.201705480.
[21] C. Madhu, B. Roy, P. Makam, T. Govindaraju, Bicomponent β-sheet assembly of dipeptide fluorophores of opposite polarity and sensitive detection of nitro-explosives, Chem. Commun. 54 (2018) 2280, https://doi.org/10.1039/C8CC00158H.
[22] H. Chen, F. Yang, Q. Chen, J. Zheng, A novel design of multi-mechanoresponsive and mechanically strong hydrogels, Adv. Mater. 29 (2017) 1606900, https://doi.org/10.1002/adma.201606900.
[23] W. Lu, M. Si, X. Le, T. Chen, Mimicking color-changing organisms to enable the multicolors and multifunctions of smart fluorescent polymeric hydrogels, Acc. Chem. Res. 55 (16) (2022) 2291–2303.
[24] Z. Li, X. Ji, H. Xie, B.Z. Tang, Aggregation-induced emission-active gels: fabrications, functions, and applications, Adv. Mater. 33 (2021) e2100021.
[25] F.F. Shen, Y. Chen, X. Xu, H.J. Yu, H. Wang, Y. Liu, Supramolecular assembly with near-infrared emission for two-photon mitochondrial targeted imaging. Small, 17 (2021) e2101185. https://doi.org/10.1002/smll.202101185.
[26] F. Yang, X. Li, Y. Chen, A chromic and near-infrared emissive mechanophore serving as a versatile force meter in micelle-hydrogel composites, Adv. Optical Mater. 10 (2022) 2102552, https://doi.org/10.1002/adom.202102552.
[27] H. Lu, J. Mack, Y. Yang, Z. Shen, Structural modification strategies for the rational design of red/NIR region BODIPYs, Chem. Soc. Rev. 43 (2014) 4778, https://doi.org/10.1039/c4cs00030g.
[28] Z. Sheng, B. Guo, D. Hu, S. Xu, W. Wu, W.H. Liew, K. Yao, J. Jiang, C. Liu, H. Zheng, B. Liu, Bright aggregation-induced-emission dots for targeted synergetic NIR-II fluorescence and NIR-I photoacoustic imaging of orthotopic brain tumors, Adv. Mater. 30 (2018) e1800766.
[29] Q. Zhao, J.Z. Sun, Red and near infrared emission materials with AIE characteristics, J. Mater. Chem. C 4 (45) (2016) 10588–10609.
[30] A. Salis, G. Rassu, M. Budai-Szűcs, I. Benzoni, E. Csányi, S. Berkó, M. Maestri, P. Dionigi, E.P. Porcu, E. Gavini, P. Giunchedi, Development of thermosensitive chitosan/glicerophospate injectable in situ gelling solutions for potential application in intraoperative fluorescence imaging and local therapy of hepatocellular carcinoma: a preliminary study, Expert Opin. Drug Deliv. 12 (10) (2015) 1583–1596.
[31] S. Li, H. Vu, J. Senkowsky, W. Hu, L. Tang, A near-infrared fluorescent pH sensing film for wound milieu pH monitoring, Exp. Dermatol. 29 (2020) 107, https://doi.org/10.1111/exd.14046.
[32] J. Liang, X. Dong, C. Wei, D. Kong, T. Liu, F. Lv, Phthalocyanine incorporated alginate hydrogel with near infrared fluorescence for non-invasive imaging monitoring in vivo, RSC Adv. 7 (2017) 6501, https://doi.org/10.1039/c6ra27756j.
[33] M. Hecht, F. Wurthner, Supramolecularly engineered J-aggregates based on perylene bisimide dyes, Acc. Chem. Res. 54 (2021) 642, https://doi.org/10.1021/acs.accounts.0c00590.
[34] C.N. Zhu, T. Bai, H. Wang, J. Ling, F. Huang, W. Hong, Q. Zheng, Z.L. Wu, Dual-encryption in a shape-memory hydrogel with tunable fluorescence and reconfigurable architecture, Adv. Mater. 33 (2021) e2102023.
[35] C.N. Zhu, T. Bai, H. Wang, W. Bai, J. Ling, J.Z. Sun, Single chromophore-based white-light-emitting hydrogel with tunable fluorescence and patternability, ACS Appl. Mater. Interfaces 10 (2018) 39343, https://doi.org/10.1002/acsami.8b12619.
[36] S. Lin, K.G. Gutierrez-Cuevas, X. Zhang, J. Guo, Q. Li, Fluorescent photochromic α-cyanodiarylethene molecular switches: an emerging and promising class of functional diarylethene, Adv. Funct. Mater. 31 (2020) 2007957, https://doi.org/10.1002/adfm.202007957.
[37] W. Lu, S. Wei, H. Shi, X. Le, G. Yin, T. Chen, Progress in aggregation-induced emission-active fluorescent polymeric hydrogels, Aggregate 2 (2021), https://doi.org/10.1002/agt2.37.
[38] S. Lin, J. Liu, X. Liu, X. Zhao, Muscle-like fatigue-resistant hydrogels by mechanical training, PNAS 116 (2019) 10244, https://doi.org/10.1073/pnas.1903019116.
[39] S. Banerjee, J.A. Kitchen, S.A. Bright, J.E. O'Brien, D.C. Williams, J.M. Kelly, T. Gunnlaugsson, Synthesis, spectroscopic and biological studies of a fluorescent Pt (II) (terpy) based 1,8-naphthalimide conjugate as a DNA targeting agent, Chem. Commun. 49 (2013) 8522, https://doi.org/10.1039/c3cc44962a.

[40] N.A. Larew, A.R. Van Wassen, K.E. Wetzel, M.M. Machala, S.D. Cummings, Solution luminescence from chloro(2,2′:6′,2″-terpyridine)platinum(II) chloride in micelles, Inorg. Chim. Acta 363 (1) (2010) 57–62.
[41] S. Hobert, J. Carney, S. Cummings, Synthesis and luminescence properties of platinum(II) complexes of 4'-chloro-2,2':6,2''-terpyridine and 4,4',4''-trichloro-2,2':6',2''-terpyridine, Inorg. Chim. Acta 318 (2001) 89, https://doi.org/10.1016/S0020-1693(01)00420-0.
[42] Q. Wei, R. Yang, D. Sun, J. Zhou, M. Li, Y. Zhang, Y. Wang, Design and evaluation of sodium alginate/polyvinyl alcohol blend hydrogel for 3D bioprinting cartilage scaffold: molecular dynamics simulation and experimental method, J. Mater. Res. Technol. 17 (2022) 66, https://doi.org/10.1016/j.jmrt.2021.12.130.
[43] Q. Rong, W. Lei, L. Chen, Y. Yin, J. Zhou, M. Liu, Anti-freezing, Conductive Self-healing Organohydrogels with Stable Strain-Sensitivity at Subzero Temperatures, Angew. Chem. Int. Ed. 56 (2017) 14159, https://doi.org/10.1002/anie.201708614.
[44] A.R. Gillies, R.L. Lieber, Structure and function of the skeletal muscle extracellular matrix, Muscle Nerve 44 (2011) 318, https://doi.org/10.1002/mus.22094.